Sensors and Actuators B 250 (2017) 461–468

Contents lists available at ScienceDirect

Sensors and Actuators B: Chemical

journal homepage: www.elsevier.com/locate/snb

Real-time monitoring of skin wound healing on nano-grooves topography using electric cell-substrate impedance sensing (ECIS)

Yao Cui, Yu An, Tongyu Jin, Fan Zhang*, Pingang He

School of Chemistry and Molecular Engineering, East China Normal University, Shanghai, 200241, PR China

ARTICLE INFO

Article history:
Received 2 February 2017
Received in revised form 19 April 2017
Accepted 27 April 2017
Available online 28 April 2017

Keywords:
Skin wound healing
Nano-grooves topography
ECIS
Cell migration
Cell proliferation

ABSTRACT

Skin wound healing represents a critical medical topic. For its ideal case, the injured tissue can repair quickly without scars. In this paper, an ECIS device was developed using nano-grooves to simulate internal extracellular matrix (ECM) with 75 nm in depth and 200 nm in width of grooves and ridges. HFF and HaCaT cells were cultured but only HFF cells could orient along the nano-grooves. In the cell migration and proliferation occurred during the wound healing, HFF and HaCaT cells both presented increased normalized impedance (NI) values at the characteristic frequencies of 977 Hz and 1465 Hz, respectively. Compared to flat electrodes, nano-grooves electrodes generated less intense impedance signals in HFF cell migration and proliferation, and HaCaT cell migration, but more intense ones in HaCaT cell proliferation. Cell images were captured simultaneously and the statistical analysis demonstrated that the nano-grooves electrode could accelerate the migration while slow down the proliferation. After establishing the correlations between impedance response and cell behaviors, it could be found that the NI values increased all linearly the rising of recovery degree and cell number. Under the equal changes of recovery degree and cell number on nano-grooves, HFF cells produced the both declined impedance signals, because of the elongation, while, HaCaT cells created the same and deduced NI variation rates, due to the unchanged morphology and aggregation growth, respectively. Our work provides a useful approach for the clinical monitoring of skin wound healing in a real-time and label-free manner, potentially promoting the development of regenerative medicine.

1. Introduction

Skin is an important protective barrier for various tissues and organs in the body that ultimately blocks foreign bodies and pathogens from entering. Skin further prevents the loss of body fluids and helps in the regulation of body temperature. Once a skin wound is generated, the dermal fibroblasts and the keratinocytes migrate to the wound and proliferate for a quick healing [1,2]. During this process, fibroblasts produce a large amount of collagen and often arrange disorderly, leading to the inevitable formation of scar tissue [3–5]. As a consequence, it is crucial to search the ways of accelerating wound healing while avoiding scar formation, as well as a method to monitor this process.

In recent decades, cell behaviors during wound healing have been investigated, however, most of them were performed on two-dimensional (2D) topographies, offering the advantages of easy operation and low cost [6,7]. However, these methods exhibit significant limitations mostly due to the differences from the environments *in vivo*. The extracellular matrix in the human body contains of various nano-scaled three-dimensional (3D) structures, which affect a series of cell behaviors [8–10]. Compared to 2D topographies, 3D topographies especially in nano-scale, may simulate the natural environment in the human body [11]. They have an obvious "contact guidance" phenomenon, in which cells could orientate along the nanostructures [12,13]. Furthermore, they could control and induce the directions and speeds of cell migration and proliferation [14–16], which plays an important role in the process of wound healing. An increasing amount of research groups have focused on the investigation of cell behaviors on various 3D topographies [17], in which fluorescence microscopy, scanning electron microscopy (SEM) and atomic force microscopy (AFM) are commonly used [18,19]. However, these methods usually involve complicated preparative steps and are often destructive to cells. More importantly, these methods rely on endpoint determination and may not provide dynamic information.

To overcome these limitations, electrical cell-substrate impedance sensing (ECIS) has gained increasing attention, since it can real-time monitor the cell behaviors non-invasively

* Corresponding author.
E-mail address: fzhang@chem.ecnu.edu.cn (F. Zhang).

http://dx.doi.org/10.1016/j.snb.2017.04.183
0925-4005/

and quantitatively [20–24]. *Giaever* and *Keese* pioneered the culture of mammalian fibroblasts on a small gold electrode [25]. When the cells attached and spread on the electrode, the current was physically impeded, resulting in an increase of impedance. Since then, cell parameters, including cell state, cell number and cell viability, have been characterized by ECIS in the study of cell attachment [26], cell proliferation [26–28], cell migration [29,30] and cell cytotoxicity [31,32]. However, ECIS monitoring has mostly been performed on 2D topographies, with few literature sources reporting impedance measurements on 3D topographies in nano-scales.

In this study, ECIS was first used to monitor the process of skin wound healing on nano-grooves topography, in which the migration and proliferation of fibroblasts (HFF cells) and keratinocytes (HaCaT cells) were investigated. Meanwhile, the correlations between impedance responses and cell behaviors were established with the assistance of microscopic analysis. Our work offers a convenient method to study the cell behavior on nano-scaled topographies, potentially promoting the development of clinical wound healing research with the purpose of accelerating skin recovery with minimal scar formation.

2. Materials and methods

2.1. Materials and reagents

Polytetrafluoroethylene (PTFE) was provided by Shanghai Plastics Research Institute (China). Polydimethylsiloxane (PDMS, Sylgard 184) was purchased from Dow Corning (Shanghai, China). Pt gauze was provided by Wuhan Gaoss Union Technology Co. Ltd., (China). Dulbecco's modified eagle's medium (DMEM), minimum essential medium (MEM), fetal bovine serum (FBS), penicillin/streptomycin (P/S), trypsin/EDTA solution, and trypan blue solution were purchased from Gibco (Shanghai, China). Glutamax, non-essential amino acids (NEAA), sodium pyruvate solution, and PBS tablets were obtained from Invitrogen (Shanghai, China). The solutions were prepared with deionized water (DI, 18.2 MΩ cm^{-1}).

2.2. Fabrication of nano-grooves topography

Nanoimprint lithography was used to produce nano-groove topography on a clean and dried glass substrate (Fig. S1). Electron beam evaporation was employed to coat a gold layer with 90 nm in thickness and a 10 nm titanium layer was also deposited as an adhesion layer between the glass slide and the gold layer. Afterwards, PMMA (polymethyl methacrylate) and nanoimprint resist (TU-7 35) were successively spin-coated on the gold substrate. Then, the nano-imprint template with 200 nm in width, 200 nm in spacing and 110 nm in depth (Beijing Huidexin Technology Co. Ltd, China), was imprinted in the resist layer using a high precision nano-imprinting machine, obtaining the transferred patterns. The residual resist layer and the underneath gold layer were removed by reactive ion etching (RIE) and inductively coupled plasma etching, respectively, followed by the removal of the remaining resist by RIE. Finally, the desired nano-grooves pattern was obtained on a gold substrate.

2.3. ECIS device assembly

The ECIS device was specially designed to facilitate simultaneous cell impedance monitoring and microscopic analysis (Fig. 1). Polytetrafluoroethylene (PTFE) was selected as the material in the manufacturing process of the cell culture chamber and baseboard due to its non-toxicity. The nano-grooves substrate with conductivity and transparence was used as working electrode (WE) with flat gold electrode as control. Pt gauze with large area was employed as counter electrode (CE) and reference electrode (RE), because of its favorable stability characteristics. The area of CE/RE and WE is 7.06 cm^2 and 0.28 cm^2, respectively, and their ratio of 25 indicated that the impedance changes were mainly caused by the working electrode, which could improve the sensitivity of measurement. To increase the tightness of device, a sealing ring made by PDMS was placed between PTFE and the working electrode. All these parts were assembled and tightened by screws.

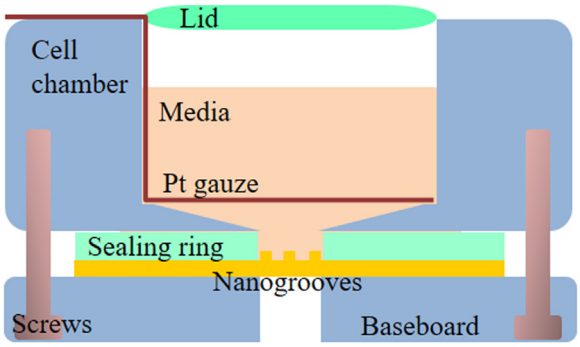

Fig. 1. Schematic representation of ECIS device configuration in the side view. The device consists of nano-grooves electrode (WE), Pt gauze (RE/CE), cell chamber, baseboard, lid and sealing ring.

Before cell seeding, all the parts of device were cleaned ultrasonically with ethyl alcohol and deionized water for 15 min, followed by the sterilization at 120 °C for 20 min and the treatment of ultraviolet light for 1 h.

2.4. Cell cultures

Human foreskin fibroblasts (HFF, Stem Cell Bank, Chinese Academy of Sciences) were cultured in DMEM supplemented with 10% FBS, 1% (P/S), 1% glutamax, 1% NEAA and 1% sodium pyruvate solution (100 mM). Human Immortal Keratinocyte Cells (HaCaT, Shanghai Bogoo Biotech Co. Ltd., China) were cultured in MEM containing 10% FBS and 1% P/S. The cells were cultured in an incubator (NuAire, USA) at 37 °C and 5% CO_2 and detached with 0.25% trypsin/EDTA at 80% confluence, followed by centrifugation (1000 rpm, 5 min) and resuspension. After staining with trypan blue and counting, the cells were seeded in the sterilized ECIS device.

2.5. Real-time impedance monitoring

In the cell migration assay, a piece of PDMS was put on the nano-grooves to isolate a thin rectangular area in an effort to simulate a wound before cell seeding [13]. HFF cells and HaCaT cells were seeded with a density of 40,000 cell/cm^2 that ensured confluence the following day. As the cells reached confluence, PDMS was took out, and the impedance was then measured within 48 h from 1 Hz to 100 kHz [33] with a signal amplitude of 10 mV using electrochemical station IGS4030 (Guangzhou Ingsens Sensor Technology Co., LTD., China). Every 12 h, the impedance signals were recorded. In order to obtain cell proliferation information, HFF and HaCaT cells were cultivated on nano-grooves with a density of 8000 cells/cm^2 for 5 days and the impedance was measured every day. In order to eliminate the influence of the medium on the impedance of the system, the culture medium was changed before impedance detection.

2.6. Microscopic analysis

An inverted fluorescence microscope (Olympus IX51, Japan) with a CCD camera was used for cell observation and images capture following impedance determination. In the migration assay,

after the removal of PDMS, cell images were captured every 12 h and this process continued for 48 h. For each moment, three images were recorded at least to calculate the mean value of the wound length. In the proliferation assay, the cells at 10 different parts of the working electrode were photographed every 24 h during 5 days and the cell number was calculated by counting the cells in the images with the expression of the mean value.

3. Results and discussion

3.1. Characterization of nano-grooves

The nano-grooves composed of alternating lines of grooves and ridges. The dimensions of the nano-grooves were characterized by scanning electron microscopy (SEM) and atomic force microscopy (AFM, Fig. S2), illustrating that the depth of the nano-grooves was approximately 75 nm and the widths of both grooves and ridges were approximately 200 nm.

3.2. Cell orientation on the nano-grooves topography

The ultimate goal of skin wound healing in clinical research is the recovery at a high rate without production of scars, in which skin fibroblasts and keratinocytes are the most significant functional cells. Thus, HFF and HaCaT cells were cultivated on the nano-grooves. As shown in Fig. 2A and B, HFF cells could be aligned along the nano-topography, while no change on HaCaT could be observed. In order to analyze the alignment quantitatively, the degree and the direction of cell elongation were evaluated based on the images captured on the 2nd day of culture, which were selected according to the cell selection principles [34,35]: The cells undercounted must be more than 300 and there is no contact between cells. Fig. 2C demonstrates that each cell is outlined manually by Photoshop and fitted to ellipse by Image J for the further analysis. The degree of elongation (E) is defined by the ratio of length and width of the cell, represented by the long and short axes of the ellipse, respectively. If $E > 4$, the cell is regarded to be elongated [35]. The direction of the elongation (θ) is expressed by the angle between long axis of the cell and nano-grooves. If $\theta < 10^\circ$, the cell is considered to be aligned along the nano-grooves [34]. The statistical data (Fig. 2D) clearly shows that 90.61% of the cells exhibit $\theta < 10^\circ$ and 8.84% of the cells feature $10^\circ < \theta < 20^\circ$. On the other hand, there are 92.27% of cells with $E > 4$ and 4.97% with $3 < E < 4$ (Fig. 2E). These results demonstrate that HFF cells have an excellent elongation and alignment performance along the nano-grooves, due to the contact guidance. It has already been reported that fibroblasts could secrete collagen during the healing process in the inflammatory response phase [36], which are always in chaotic arrangement, leading to the formation of scar tissue [3,4]. While, cell alignment may contribute to the ordered arrangement of collagen, thus reducing the formation of scars to some degree.

3.3. Cell migration assay

The wound healing process mainly involves the migration and proliferation of fibroblasts and keratinocytes [2]. The combination effect of these two cell types enables the wound to heal in time. Therefore, studying the contributions of migration and proliferation respectively for wound healing is highly relevant.

In the cell migration assay, ECIS was employed to monitor the respective impedance responses of HFF and HaCaT cells on the nano-grooves during the recovery of a wound. From Fig. 3A and B, it can be observed that the impedance increased continuously with time for the two cell types within 48 h. It is well known that ECIS is

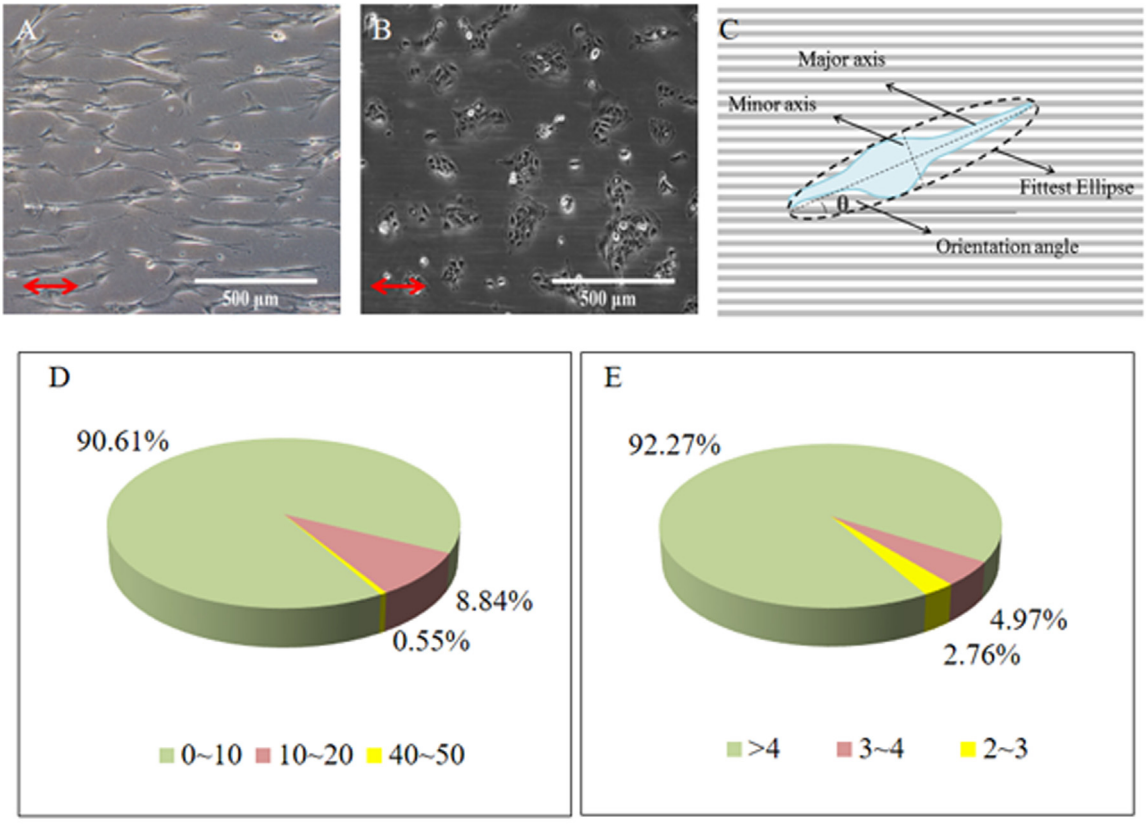

Fig. 2. HFF cells (A) and HaCaT cells (B) cultivated on nano-grooves electrodes at a density of 8000 cells/cm^2, schematic representation of cell parameters (C), and statistical data of alignment angle θ (D) and E value (E) for HFF cells on nano-grooves.

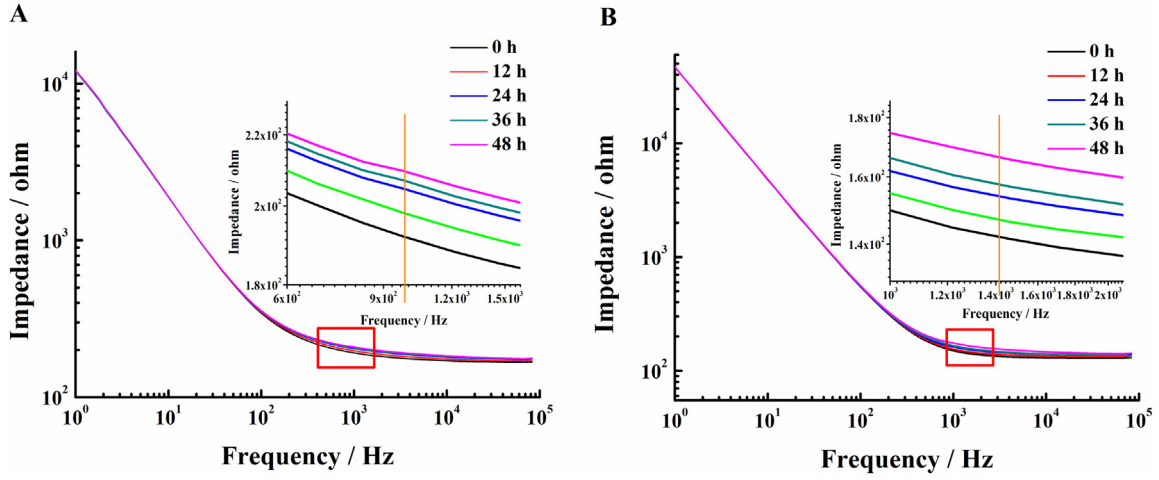

Fig. 3. Bode plot for the migration of HFF cells (A) and HaCaT cells (B) within 48 h on nano-grooves.

a frequency-dependent method. In order to improve the monitoring sensitivity, 977 Hz and 1465 Hz were selected as characteristic frequencies for HFF and HaCaT cells, at which the corresponding impedance differed the most. In order to allow for a more uniform comparison of impedance between the electrodes and between experiments, the impedance with cells at each point was normalized by the initial impedance of culture medium without cells, obtaining the normalized impedance (NI) [31]:

$$NI = \frac{Z_{cell} - Z_{cell-free}}{Z_{cell-free}}, \quad (1)$$

where Z_{cell} and $Z_{cell\text{-}free}$ represent the impedance of the system with and without cells in the device at the same conditions, respectively.

Fig. 4A shows the NI value changes of HFF cells in the migration process during wound healing on the nano-grooves and flat electrodes as control. With the prolongation of migration time, NI value increases from 0 to 0.0554 on the nano-grooves electrode and from 0 to 0.1145 on the flat electrode, indicating that HFF cells on the nano-grooves electrodes produce smaller impedance signal with declined increasing speed, compared to flat electrodes. For HaCaT cells, the NI values change from 0 to 0.0490 and 0.0377 on the nano-grooves and flat electrodes, respectively (Fig. 4B), which shows that the impedance response of HaCaT cells is stronger on the nano-grooves with the improved increasing rate.

The impedance signals and their variation reflects the healing degree. Thus, it is very important to establish the correlations between these two variables for a broader application of ECIS in clinical settings without the observation, the wound was imaged after impedance determination. Fig. S3 illustrates that after the wound formation, HFF cells migrate to the wound and are nearly converged at 48 h on both electrodes even with the different initial wound gap. Similarly, the migration of HaCaT cells in 48 h causes the almost confluence, although the nano-grooves electrode exhibits a larger initial uncovered area than the flat electrode. In detail, the wound length (L) decreases 3759 μm and 2666 μm on the nano-grooves and flat electrode, respectively, attributed by the migration of HFF cells (Fig. 4C). The results present an increase in migration speed, due to the elongation and alignment of fibroblasts along the nano-grooves electrodes. In parallel, HaCaT cells migrate 3411 μm and 2190 μm on the nano-grooves and flat electrode, respectively (Fig. 4D), indicating that the nano-grooves could also accelerate the migration of keratinocytes, even with no effect on the cell morphology. Therefore, it can be concluded that the nano-grooves topography may indeed improve the performance of cell migration. Based on these data, the degree of wound healing, represented by the recovery degree (R)% could be calculated as follows:

$$R(\%) = (L_0 - L_t)/L_0 \quad (2)$$

where L_0 is the initial length of wound and L_t is the length at a determination moment [37].

As indicated in Fig. 4E and F, there is a good linear correlation between the NI value and the recovery degree for both HFF and HaCaT cells, irrespective of the electrode type (flat or nano-grooves). The correlations for HFF cells could be expressed as $NI = 5.51 \times 10^{-4} \times R(\%) + 5.52 \times 10^{-4}$ with linear regression coefficient $R = 0.999$ on the nano-grooves electrode, and $NI = 1.18 \times 10^{-3} \times R(\%) - 9.01 \times 10^{-4}$ with linear regression coefficient $R = 0.996$ on the flat electrode. For HaCaT cells, the NI value is correlated with the recovery degree using the equations of $NI = 5.10 \times 10^{-4} \times R(\%) + 3.07 \times 10^{-4}$ with a linear regression coefficient $R = 0.998$ on the nano-grooves electrode and $NI = 5.20 \times 10^{-4} \times R(\%) - 1.83 \times 10^{-4}$ with a linear regression coefficient of $R = 0.999$ on the flat electrode. Derived from these quantitative correlations, as the wound healed at the same percentage, the NI value of HFF cells changes more slowly on the nano-grooves than the flat electrode, while, HaCaT cells display the almost same variation of the NI value on both electrodes. Hypotheses are that HFF cells are elongated by the nano-grooves, thus covering a smaller area compared to the flat surface upon healing the wound at the same percentage, while, no influence on HaCaT cell morphology by the nano-grooves generate the equal covered areas. However, it is worth noting that wound healing at the same percentage on the nano-grooves takes less time in this context. Consequently, the NI value may reflect the wound healing degree to some extent.

3.4. Cell proliferation assay

In addition to cell migration, proliferation is another significant factor in skin wound healing. The behaviors of HFF cells and HaCaT cells in the proliferation process were determined by ECIS in 5 days on the nano-grooves electrode with a flat electrode as control (Fig. 5). Fig. 6A shows the NI values of HFF cells at 977 Hz, caused by the cell proliferation during the wound healing on nano-grooves and flat electrodes with the increment of 0.1967 and 0.2396, respectively. The trend of NI increase on the two electrode types is basically the same: fast increase in the beginning while consistently slowing down thereafter. But, the NI value of the nano-grooves electrode grows more slowly than that of the flat electrode, ulti-

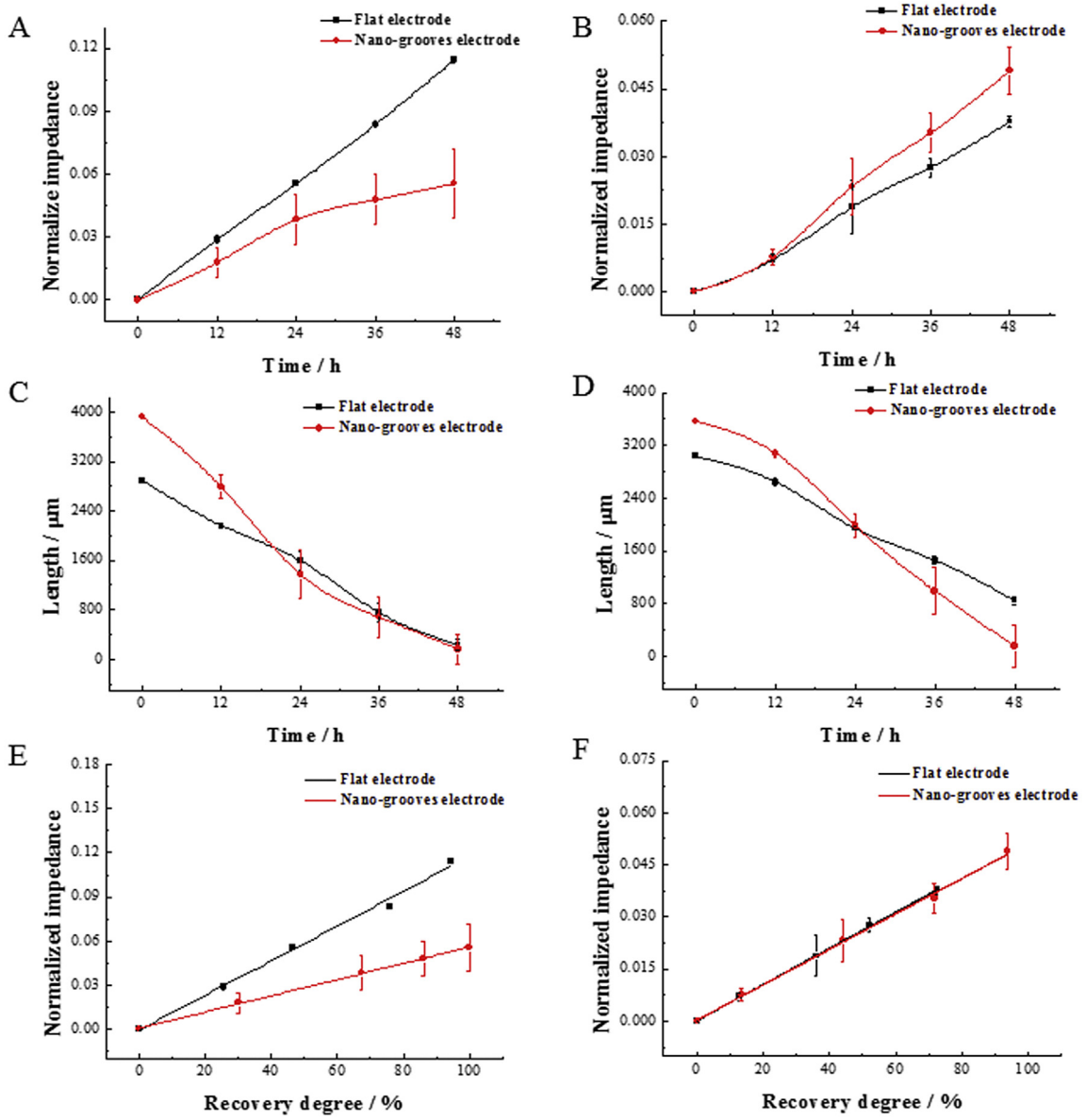

Fig. 4. NI curves in the migration assay within 48 h for HFF cells at 977 Hz (A) and HaCaT cells at 1465 Hz (B), variation of wound length over time for HFF cells (C) and HaCaT cells (D), and linear correlation between NI value and recovery degree for HFF cells (E) and HaCaT cells (F) on the nano-grooves and flat electrodes.

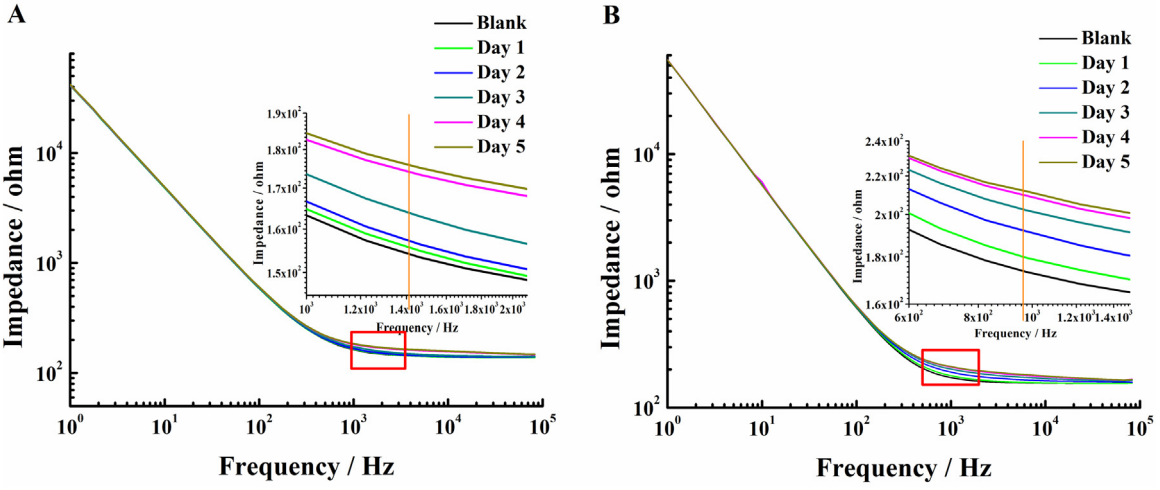

Fig. 5. Bode plot for the proliferation of HFF cells (A) and HaCaT cells (B) within 5 days on nano-grooves.

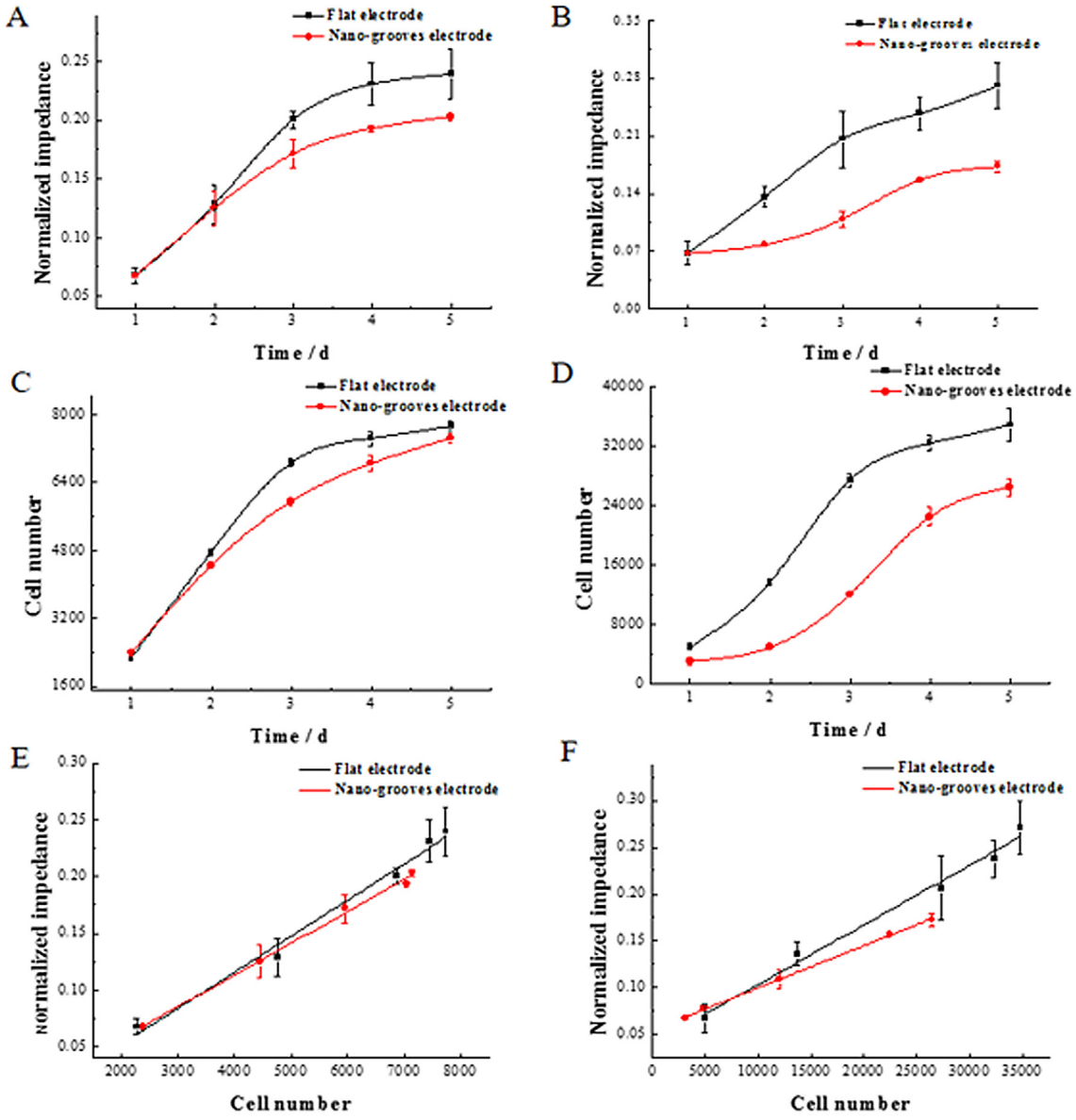

Fig. 6. NI curves in the proliferation assay within 5 days for HFF cells at 977 Hz (A) and HaCaT cells at 1465 Hz (B), variation of cell number over time for HFF cells (C) and HaCaT cells (D), and linear correlation between normalized impedance and cell number for HFF cells (E) and HaCaT cells (F) on nano-grooves and flat electrodes.

mately resulting in a lower final NI value. For HaCaT cells, the NI values increase over time on both electrodes. However, the overall growth rate on the nano-grooves is much smaller, compared to the flat electrode (Fig. 6B).

From the photographs taken after the impedance measurements (Fig. S4), it could be observed that the number of both HFF and HaCaT cells increases with the proceeding of cell proliferation on both nano-grooves and flat electrodes. The statistical data in Fig. 6C show that the number of HFF cells on nano-grooves is smaller over 5 days. However, from Day 1 to Day 3, cell proliferate in lower rate, while, in the later 2 days, cell number increases faster in comparison with that on flat electrode. As mentioned above, HFF cells could be elongated and aligned along the nano-grooves, thus leading to the aligned cell division. Meanwhile, the division in the other directions is deduced to be limited. Consequently, in the first 3 days, cell proliferation along the nano-grooves would cause the earlier appearance of "contact inhibition" effect compared to that on flat electrodes, resulting in the declined cell growth rate. During the later period, in spite of the contact inhibition along the nano-grooves, there are still relatively many uncovered areas for cell proliferation, thus the increasing rate of cell number is not reduced too much. While, the cells on the flat surface would be divided in random directions, leading to a faster increasing number. Once the contact inhibition occurs, the cell would proliferate in a much declined rate. HaCaT cells exhibit the similar variation trends (Fig. 6D), but with much more obvious distinction between the two types of surface, most likely because the nano-grooves are not suitable for HaCaT cell growth. The results obtained suggest that the proliferation of both HFF and HaCaT cells are reduced on the nano-grooves electrode. It is known that HFF cells secreting collagen are the main cell type to cause scarring. The slowed HFF cell proliferation could bring about the reduction of collagen, avoiding an excessive accumulation around the wound site. Therefore, the nano-grooves topography exhibits a positive effect on the reduction of scar tissue.

Fig. 6E and F highlights the correlations between NI values and the cell numbers in the proliferation process. The good linearity of HFF cells could be presented by equations of $NI = 2.79 \times 10^{-5} \times N(\text{cells}) + 1.42 \times 10^{-3}$ with a linear regression coefficient of R = 0.998 on the nano-grooves electrode and $NI = 3.18 \times 10^{-5} \times N(\text{cells}) - 1.18 \times 10^{-2}$ with a linear regression coefficient of R = 0.992 on the flat electrode. For HaCaT cells, the linear correlations could be expressed as $NI = 4.49 \times 10^{-6} \times N(\text{cells}) + 5.51 \times 10^{-2}$ with a linear regression coefficient of R = 0.999 on the nano-grooves electrode and $NI = 6.35 \times 10^{-6} \times N(\text{cells}) + 3.99 \times 10^{-2}$, with a linear regression coefficient of R = 0.996 on the flat electrode. The relatively smaller slope on the nano-grooves could indicate the less increment of NI value under the same change of cell number, since the elongated HFF cells and the clustered HaCaT cells probably both occupy a smaller area, compared to the cells with normal morphology on the flat surface. These correlations show that the impedance response could represent the cell number to a certain degree. As such, it is possible to extend the impedance monitoring into the field of clinic research.

4. Conclusions

In this study, electric cell-substrate impedance sensing (ECIS) was used for the first time to monitor the process of skin wound healing on the nano-grooves topography with dimensions of 75 nm in depth and 200 nm in width, simulating the internal ECM. HFF and HaCaT cells, belonging to the fibroblasts and keratinocytes, respectively, participate mainly in skin wound healing, were cultivated on the nano-grooves electrodes, and HFF cells are found to be elongated and aligned along the nano-grooves. Skin wound healing includes cell migration and cell proliferation. In the former process, NI values of HFF and HaCaT cells at their characteristic frequency of 977 Hz and 1465 Hz, respectively, increase with the prolongation of migration time during 48 h. However, HFF cells on the nano-grooves generate a greater NI value variation than the flat electrode, while HaCaT cells show an opposite trend. With the assistance of microscopic analysis, indicating that nano-grooves electrodes could accelerate the speed of two cell types, NI values were correlated with recovery degree linearly. The results obtained show that at the same healing percentages, the nano-grooves electrode caused less NI value change for HFF cells, probably due to the elongated morphology on the nano-grooves. While for HaCaT cells, the NI value changes are almost identical, since there is most likely no difference in the cell morphology between the nano-grooves and flat electrodes. In cell proliferation experiments, the NI values within 5 days for both HFF and HaCaT cells present a sustainable increase over time on the nano-grooves electrodes, however, a slower increase than on the flat electrodes could be determined. Microscopic analysis indicates that HFF and HaCaT cells feature a reduced proliferation rate on the nano-grooves electrode. The linear correlation between the NI value and the cell number could be established, indicating that the same number increasing of HFF cells on the nano-grooves induces less NI value change than flat electrode. This finding is likely due to the fact that HFF cells were elongated on the nano-grooves, thus occupying a smaller area. HaCaT cells show the same comparison results as well. However, the reason is that the cells grow in clusters. In summary, the accelerated migration and slowed proliferation of HFF and HaCaT cells on the nano-grooves could contribute to a faster recovery of skin wound with reduced formation of scar tissue. The establishment of the correlation between impedance response and cell behaviors related to the wound healing shows the significance in the applications of ECIS to label-free and real-time monitoring of the clinical skin wound healing process.

Acknowledgement

This work was supported by the National Nature Science Foundation of China (Grant No. 21405049).

Appendix A. Supplementary data

Supplementary data associated with this article can be found, in the online version, at http://dx.doi.org/10.1016/j.snb.2017.04.183.

References

[1] B. Bandyopadhyay, J.H. Fan, S.X. Guan, Y. Li, M. Chen, D.T. Woodley, W. Li, A traffic control role for TGF beta 3: orchestrating dermal and epidermal cell motility during wound healing, J. Cell Biol. 172 (2006) 1093–1105.
[2] P. Martin, Wound healing – aiming for perfect skin regeneration, Science 276 (1997) 75–81.
[3] H.P. Ehrlich, T.M. Krummel, Regulation of wound healing from a connective tissue perspective, Wound Repair Regen. 4 (1996) 203–210.
[4] F.W. Frantz, R.F. Diegelmann, B.A. Mast, I.K. Cohen, Biology of fetal wound healing: collagen biosynthesis during dermal repair, J. Pediatr. Surg. 27 (1992) 945–949.
[5] M. David-Raoudi, F. Tranchepain, B. Deschrevel, J.-C. Vincent, P. Bogdanowicz, K. Boumediene, J.-P. Pujol, Differential effects of hyaluronan and its fragments on fibroblasts: relation to wound healing, Wound Repair Regen. 16 (2008) 274–287.
[6] Y. Zhang, G. Yu, Y. Xiang, J. Wu, P. Jiang, W. Lee, Y. Zhang, Bm-TFF2 a toad trefoil factor, promotes cell migration, survival and wound healing, Biochem. Biophys. Res. Commun. 398 (2010) 559–564.
[7] C.R. Keese, J. Wegener, S.R. Walker, L. Giaever, Electrical wound-healing assay for cells in vitro, PNAS 101 (2004) 1554–1559.
[8] S. Patel, K. Kurpinski, R. Quigley, H. Gao, B.S. Hsiao, M.-M. Poo, S. Li, Bioactive nanofibers: synergistic effects of nanotopography and chemical signaling on cell guidance, Nano Lett. 7 (2007) 2122–2128.
[9] L. Yildirimer, N.T.K. Thanh, A.M. Seifalian, Skin regeneration scaffolds: a multimodal bottom-up approach, Trends Biotechnol. 30 (2012) 638–648.
[10] I. Tonazzini, E. Jacchetti, S. Meucci, F. Beltram, M. Cecchini, Schwann cell contact guidance versus boundary interaction in functional wound healing along nano and microstructured membranes, Adv. Healthcare Mater. 4 (2015) 1849–1860.
[11] K. von der Mark, J. Park, S. Bauer, P. Schmuki, Nanoscale engineering of biomimetic surfaces: cues from the extracellular matrix, Cell Tissue Res. 339 (2010) 131–153.
[12] R.G. Flemming, C.J. Murphy, G.A. Abrams, S.L. Goodman, P.F. Nealey, Effects of synthetic micro- and nano-structured surfaces on cell behavior, Biomaterials 20 (1999) 573–588.
[13] K. Hong Nam, H. Yoonmi, K. Min Sung, K. Sun Min, S. Kahp-Yang, Effect of orientation and density of nanotopography in dermal wound healing, Biomaterials 33 (2012) 8782–8792.
[14] J.Y. Li, Y.C. Ho, Y.C. Chung, F.C. Lin, W.L. Liao, W.B. Tsai, Preparation of micron/submicron hybrid patterns via a two-stage UV–imprint technique and their dimensional effects on cell adhesion and alignment, Biofabrication 5 (2013) 1–13.
[15] Q. Zhang, H. Dong, Y. Li, Y. Zhu, L. Zeng, H. Gao, B. Yuan, X. Chen, C. Mao, Microgrooved polymer substrates promote collective cell migration to accelerate fracture healing in an in vitro model, ACS Appl. Mater. Inter. 7 (2015) 23336–23345.
[16] E.K.F. Yim, R.M. Reano, S.W. Pang, A.F. Yee, C.S. Chen, K.W. Leong, Nanopattern-induced changes in morphology and motility of smooth muscle cells, Biomaterials 26 (2005) 5405–5413.
[17] C.J. Bettinger, R. Langer, J.T. Borenstein, Engineering substrate topography at the micro- and nanoscale to control cell function, Angew. Chem. Int. Edit. 48 (2009) 5406–5415.
[18] B.S. Zhu, Q.Q. Zhang, Q.H. Lu, Y.H. Xu, J. Yin, J. Hu, Z. Wang, Nanotopographical guidance of C6 glioma cell alignment and oriented growth, Biomaterials 25 (2004) 4215–4223.
[19] X. Zhou, J. Hu, J. Li, J. Shi, Y. Chen, Patterning of two-level topographic cues for observation of competitive guidance of cell alignment, ACS Appl. Mater. Inter. 4 (2012) 3888–3892.
[20] W. Gu, Y. Zhao, Cellular electrical impedance spectroscopy: an emerging technology of microscale biosensors, Expert Rev. Med. Devices 7 (2010) 767–779.
[21] R. Eldawud, A. Wagner, C. Dong, Y. Rojansakul, C.Z. Dinu, Electronic platform for real-time multi-parametric analysis of cellular behavior post-exposure to single-walled carbon nanotubes, Biosens. Bioelectron. 71 (2015) 269–277.
[22] Y. Qiu, R. Liao, X. Zhang, Real-time monitoring primary cardiomyocyte adhesion based on electrochemical impedance spectroscopy and electrical cell-substrate impedance sensing, Anal. Chem. 80 (2008) 990–996.
[23] J. Wegener, C.R. Keese, I. Giaever, Electric cell-substrate impedance sensing (ECIS) as a noninvasive means to monitor the kinetics of cell spreading to artificial surfaces, Exp. Cell Res. 259 (2000) 158–166.

[24] P. Daza, A. Olmo, D. Canete, A. Yufera, Monitoring living cell assays with bio-impedance sensors, Sens. Actuators B-Chem. 176 (2013) 605–610.
[25] I. Giaever, C.R. Keese, Micromotion of mammalian cells measured electrically, PNAS 88 (1991) 7896–7900.
[26] C. Xiao, B. Lachance, G. Sunahara, J.H.T. Luong, An in-depth analysis of electric cell-substrate impedance sensing to study the attachment and spreading mammalian cells, Anal. Chem. 74 (2002) 1333–1339.
[27] L. Wang, H. Yin, W. Xing, Z. Yu, M. Guo, J. Cheng, Real-time, label-free monitoring of the cell cycle with a cellular impedance sensing chip, Biosens. Bioelectron. 25 (2010) 990–995.
[28] L. Yang, L.R. Arias, T.S. Lane, M.D. Yancey, J. Mamouni, Real-time electrical impedance-based measurement to distinguish oral cancer cells and non-cancer oral epithelial cells, Anal. Bioanal. Chem. 399 (2011) 1823–1833.
[29] L. Wang, J. Zhu, C. Deng, W.-I. Xing, J. Cheng, An automatic and quantitative on-chip cell migration assay using self-assembled monolayers combined with real-time cellular impedance sensing, Lab Chip 8 (2008) 872–878.
[30] W. Gamal, S. Borooah, S. Smith, I. Underwood, V. Srsen, S. Chandran, P.O. Bagnaninchi, B. Dhillon, Real-time quantitative monitoring of hiPSC-based model of macular degeneration on electric cell-substrate impedance sensing microelectrodes, Biosens. Bioelectron. 71 (2015) 445–455.
[31] T.M. Curtis, M.W. Widder, L.M. Brennan, S.J. Schwager, W.H. van der Schalie, J. Fey, N. Salazar, A portable cell-based impedance sensor for toxicity testing of drinking water, Lab Chip 9 (2009) 2176–2183.
[32] F. Asphahani, M. Zhang, Cellular impedance biosensors for drug screening and toxin detection, Analyst 132 (2007) 835–841.
[33] R. Pradhan, M. Mandal, A. Mitra, S. Das, Monitoring cellular activities of cancer cells using impedance sensing devices, Sens. Actuators B-Chem. 193 (2014) 478–483.
[34] P.F. Nealey, C.J. Murphy, A.I. Teixeira, G.A. McKie, J.D. Foley, P.J. Bertics, The effect of environmental factors on the response of human corneal epithelial cells to nanoscale substrate topography, Biomaterials 27 (2006) 3945–3954.
[35] E.K.F. Yim, S.W. Pang, K.W. Leong, Synthetic nanostructures inducing differentiation of human mesenchymal stem cells into neuronal lineage, Exp. Cell Res. 313 (2007) 1820–1829.
[36] A. Young, C.-E. McNaught, The physiology of wound healing, Surgery 29 (2011) 475–479.
[37] J.M. Yang, S.-W. Chen, J.-H. Yang, C.-C. Hsu, J.-S. Wang, A quantitative cell modeling and wound-healing analysis based on the Electric Cell-substrate Impedance Sensing (ECIS) method, Comput. Biol. Med. 69 (2016) 134–143.

Biographies

Yao Cui obtained the B.S. degree in Chemistry at Hebei Normal University (Hebei, China) in 2014. She is currently working towards her M.S. degree in Analytical Chemistry at East China Normal University (Shanghai, China) in 2017. Her research interests are the design and fabrication of micro- and nano-electrodes and the impedance monitoring of cell behaviors.

Yu An received the B.S. degree in Chemistry at Shanxi University (Shanxi, China) in 2015. She is currently working towards her PhD degree in Analytical Chemistry at East China Normal University (Shanghai, China). Her interests include cellular impedance measurement for profiling cytotoxicity.

Tongyu Jin received the B.S. degree in Chemistry at East China University of Science and Technology (Shanghai, China) in 2016. She is expecting to receive her M.S. degree in Analytical Chemistry at East China Normal University (Shanghai, China) in 2019. Her research interest is the impedance monitoring of cell behaviors.

Fan Zhang received her M.S. degree in Analytical Chemistry at the Department of Chemistry in East China Normal University (Shanghai, China) in 2008. From 2008 to 2011, she worked as a jointly supervised Ph.D. student at the Department of Chemistry in Ecole Normale Supérieure (Paris, France) and East China Normal University (Shanghai, China). Now she is working at the Department of Chemistry in East China Normal University (Shanghai, China) as lecturer. Her research interests include the development of microfluidic devices and micro/nano electrodes, and the study of electric and electrochemical responses of cells.

Pingang He is Vice Secretary-General of Electrochemical Instrument Committee in China Instrument and Control Society, Director of Analytical Chemistry Committee in Shanghai Society of Chemistry and Chemical Industry, and East China Normal University-Branch President of Shanghai Oversea Returned Scholars Association. He received his Ph.D. degree from Fudan University (Shanghai, China) in 1996. Since 1998 he has been working as professor in East China Normal University (Shanghai, China). His research interests include biosensors, preparation and application of nano-materials, electrochemistry/in situ electrochemistry of scanning probe, capillary electrophoresis/electrochemical detection, novel electrochemical analytical instrument.